A critical evaluation of GGA plus U modeling for atomic, electronic and magnetic structure of Cr2AlC, Cr2GaC and Cr2GeC

Martin Dahlqvist, Björn Alling and Johanna Rosén

Original Publication:

Martin Dahlqvist, Björn Alling and Johanna Rosén, A critical evaluation of GGA plus U modeling for atomic, electronic and magnetic structure of Cr2AlC, Cr2GaC and Cr2GeC, 2015, Journal of Physics: Condensed Matter, (27), 9, 095601.
http://dx.doi.org/10.1088/0953-8984/27/9/095601

A critical evaluation of GGA+*U* modeling for atomic, electronic, and magnetic structure of Cr_2AlC, Cr_2GaC, and Cr_2GeC

M. Dahlqvist*, B. Alling, and J. Rosen

Thin Film Physics, Department of Physics, Chemistry, and Biology (IFM), Linköping University, SE-581 83 Linköping, Sweden

* Electronic mail: madah@ifm.liu.se

In this work we critically evaluate methods for treating electrons correlation effects in multicomponent carbides using a GGA+*U* framework, addressing doubts from previous works on the usability of density functional theory in the design of magnetic MAX phases. We have studied the influence of the Hubbard *U*-parameter, applied to Cr 3*d* orbitals, on the calculated lattice parameters, magnetic moments, magnetic order, bulk modulus, and electronic density of states of Cr_2AlC, Cr_2GaC, and Cr_2GeC. By considering non-, ferro-, and five different antiferromagnetic spin configurations, we show the importance of including a broad range of magnetic orders in the search for MAX-phases with finite magnetic moments in the ground state. We show that when electron correlation is treated on the level of the generalized gradient approximation (U = 0 eV), the magnetic ground state of Cr_2AC (A = Al, Ga, Ge) is in-plane antiferromagnetic with finite Cr local moments, and calculated lattice parameters and bulk modulus close to experimentally reported values. By comparing GGA and GGA+*U* results with experimental data we find that using a *U*-value larger than 1 eV results in structural parameters deviating strongly from experimentally observed values. Comparisons are also done with hybrid functional calculations (HSE06) resulting in an exchange splitting larger than what is obtained for a *U*-value of 2 eV. Our results suggest caution and that investigations need to involve several different magnetic orders before lack of magnetism in calculations are blamed on the exchange-correlation approximations in this class of magnetic MAX phases.

1. Introduction

Conventional density functional theory (DFT) within the local density approximation (LDA) and the generalized gradient approximation (GGA) poorly describes strongly correlated electron materials, e.g. transition metal oxides and nitrides [1-6]. as the electrons are incorrectly overdelocalized which results in an inaccurate description of relative energies, magnetic ground states, and electronic structure (converts what should be an insulator to a metal). In fact, for such materials the many electrons in partially filled *d* or *f* orbitals are inherently localized on each metal atom. By introducing the on-site Coulomb repulsion *U* applied to localized electrons like 3*d* or 4*f*, i.e. DFT+*U* approaches, results are improved [7-10]. However, for compounds with delocalized states, e.g. intermetallic phases and transition metal carbides, the use of ordinary LDA and GGA give good results. The question is what exchange-correlation approximations are the most reliable for investigations of Cr_2AC (*A* = Al, Ga, Ge) phases?

Cr_2AC belong to a group of inherently nanolaminated thermodynamically stable materials known as the $M_{n+1}AX_n$ (MAX) phases (n = 1 – 3). These are comprised of transition metal (*M*) carbide or nitride (*X*) sheets ($M_{n+1}X_n$) interleaved by a single layer of an *A*-group element [11, 12]. For n = 1, the hexagonal structure, which belongs to the $P6_3/mmc$ space group, give a *M-X-M-A-M-X-M-A* atomic layer stacking in the *c* direction ([0001]). The MAX phases combine ceramic and metallic characteristics, and with suggested tunable anisotropic transport properties [13] in combination with magnetism, they may have potential as functional materials within, e.g., sensor and spintronics applications. Moreover, layered magnetic materials are attractive for fundamental physics investigations and applications exploiting the spin rather than the charge of the electrons, such as for giant magnetoresistance (GMR) effects [14].

Inspired by our theoretical prediction [15], magnetism has now been observed experimentally in MAX phase materials [16-24]. Up to date, a few different MAX phases experimentally indicate ferri- or ferromagnetic (FM) behaviour [16-19, 21-23]. Alloying Cr-based MAX phases with Mn results in a magnetic state depending on composition [16, 19, 23], where $(Cr_{0.75}Mn_{0.25})_2GeC$ display FM response up to at least 300 K [16]. Most recently, a MAX phase with Mn as sole *M*-element (Mn_2GaC) was also synthesized as a heteroepitaxial thin film, with FM response up to 230 K [17].

Even though the Cr based MAX phases Cr_2AlC, Cr_2GaC, and Cr_2GeC are vital in providing phase stability and a retained structure upon magnetization through alloying with Mn, their respective inherent magnetic ground state, if any, are not unambiguously identified. Further understanding of the magnetic ground states and associated transitions are required for these virgin materials, to enable improved understanding of the effects of alloying, and, in turn, potentially allow tuning of their magnetic properties.

Theoretical studies of magnetic MAX phases often include only non-magnetic (NM), FM, and one antiferromagnetic (AFM) state [25-33]. The descriptions in the literature of the AFM states considered are often vague, but may be interpreted as alternating *M*-layers of spin up and spin down, possible to fit into a single MAX phase unit cell. Furthermore, different approaches in terms of electron correlations beyond the standard LDA and GGA functionals have been considered, in particular including an additional and adjustable Hubbard *U*-term [28, 29, 31-34]. By doing so, both FM and AFM ground states have been theoretically predicted for Cr_2AlC and Cr_2GeC with a magnetic moment between 0.01 and 1.79 μ_B per Cr atom [28, 29, 31-33]. This can be compared to experimentally measured magnetic moment of only ~0.002 and ~0.05 μ_B per Cr atom in Cr_2AlC, and with a transition temperature of 73 K, interpreted as very weak FM or canted AFM spin configuration [18, 24]. However, any motivation why one needs to use +*U* approaches, in terms of physical reasons, is rarely seen. It is well known that GGA+*U* works reasonably well for strongly correlated materials like transition metal oxides and nitrides. The question is if electron correlations in MAX phases in general, and Cr_2AC in particular, are strong enough that +*U* methods are required. This double uncertainty, both of the nature of the magnetic ground states and the question if strong electron correlations needs to be considered or not, has caused doubts on the usability of first-principles calculations in the development of magnetic MAX phases.

In this study we address these questions using first-principles density functional theory (DFT) to search for the magnetic ground state of Cr_2AlC, Cr_2GaC, and Cr_2GeC. We include NM, FM, and multiple AFM configurations, also comprising AFM states with anti-parallel spins within the Cr-layers. Simultaneously, we also explore the effect of electron correlation approximation on predicted magnetic ground state, crystal structure, and bulk modulus. We show that both the magnetic configurations as well as how the electron correlation effects are approximated have an impact on the calculated results. We discuss the findings and the suitability of the approximation in a comparison with experimental results.

2. Computational details

For the 1×1×1 unit cell (8 atoms), three AFM configurations were considered: single layer AFM with spins changing sign for every *M*-atom layer, corresponding to the $\mathrm{AFM}[0001]_1$ spin configuration, and double layer AFM ordering with two consecutive *M*-layers with the same spin direction, before changing sign upon crossing an *A* or *X* layer ($\mathrm{AFM}[0001]_2^A$ and $\mathrm{AFM}[0001]_2^X$, respectively). In order to allow for AFM configurations with antiparallel spins within one *M*-layer, 2×1×1 unit cells are required (in-AFM1 and in-AFM2). All considered spin configurations are illustrated in Fig. 1. Details of their crystal structure with specified spin configuration can be found in Appendix.

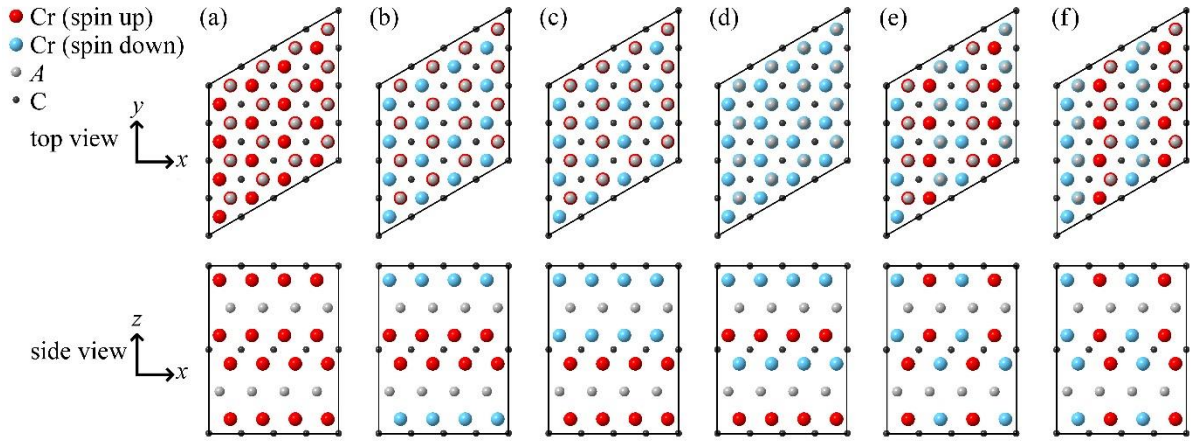

Figure 1. (Color online) Schematic illustration of six ordered collinear magnetic structures considered for Cr2*A*C where (a) is FM, (b) AFM$[0001]_2^A$, (c) AFM$[0001]_2^X$, (d) AFM$[0001]_1$, (e) in-AFM1, and (f) in-AFM2. To clearly distinct the different AFM configurations they are represented by a supercell consisting of 4×4×1 unit cells (128 atoms in total).

Our DFT calculations were performed using the projector augmented wave (PAW) [35] method as implemented within the Vienna *ab-initio* simulation package (VASP) [36, 37]. We have used the generalized gradient approximation (GGA) as parameterized by Perdew,Burke, and Ernzerhof (PBE) in its spin-polarized form [38, 39]. In addition we also used the rotationally invariant approach to GGA+*U*, applied onto the Cr 3*d* electrons, as proposed by Dudarev [8, 40]. In this formalism the onsite Coulomb parameter *U* and the exchange parameter *J* are combined into a spherically averaged, single effective interaction parameter, $U - J$, which does not depend on their individual values. In the following we will refer to this effective interaction parameter as U_{eff}. We have also performed hybrid exchange-correlation functional calculations (HSE06) with a screening parameter μ of 0.2 Å^{-1} [41-43]. The magnetic moments are calculated by projecting the plane-wave states into the PAW spheres of the Cr atoms.

We have performed the reciprocal-space integration within the Monkhorst-Pack scheme [44] with 23×23×7 and 13×23×7 *k*-point mesh for 1×1×1 and 2×1×1 unit cells, respectively, together with a plane-wave cutoff energy of 400 eV. The calculated total energies were converged within 0.1 meV/atom in terms of *k*-point sampling and cutoff energy. Cr_2AC phases were relaxed in terms of unit-cell volumes, c/a ratios, and internal parameters in order to minimize the total energy. The structures were considered to be converged with respect to ionic displacements when the total energy difference between two ionic steps were less than 0.02 meV/atom and the forces acting on the atoms were smaller than 0.02 eV/Å. Bulk modulus B_0 was determined by fitting the energy-volume curves with a Birch-Murnaghan equation of state.

3. Results and discussion

A comparison of the relative energies for all here considered magnetic states of Cr_2AC (A = Al, Ga, Ge) is presented in figure 1(a - c), for which no correlation of the Cr d electrons beyond the GGA is applied, i.e. U_{eff} = 0 eV. The energy for each spin configuration is given relative to the NM energy minimum, E_0^{NM}, as calculated by $\Delta E(V) = E(V) - E_0^{NM}(V_0)$. For both Cr_2AlC and Cr_2GaC all magnetic states but in-AFM1 are close to degenerate with the NM configuration. Cr_2GeC, on the other hand, show three magnetic states clearly distinct from NM, i.e. AFM$[0001]_2^X$, in-AFM1, and in-AFM2. Still, for all three Cr_2AC phases, the in-AFM1 is found to have lowest energy, -3 meV/atom for Cr_2AlC, -4 meV/atom for Cr_2GaC, and -8 meV/atom for Cr_2GeC, respectively, where the latter is -4 meV/atom relative to AFM$[0001]_2^X$.

Figure 2(d - f) shows the energy of different magnetic configurations of Cr_2AC (A = Al, Ga, Ge) relative to the NM state for exchange correlations approximations with U_{eff} equal to 0, 1 and 2. The energy is hence given by $\Delta E(U_{eff}) = E_0^{mag}(U_{eff}) - E_0^{NM}(U_{eff})$, where $E_0^{mag}(U_{eff})$ and $E_0^{NM}(U_{eff})$ are the equilibrium total energies of the magnetic and NM states, respectively, for a given value of U_{eff}. The details for U_{eff} = 0 is also shown in panel (a - c). For U_{eff} = 1 eV the magnetic states are, in general, no longer degenerate with NM. All Cr_2AC display a clear spread in ΔE. Again, in-AFM1 is found as the magnetic state of lowest energy with ΔE = -32, -43, and -55 meV/atom for A = Al, Ga, Ge, respectively.

Since most magnetic states are no longer degenerate with NM, an assessment of the ground state can be improved by comparing in-AFM1 with the second most stable state, i.e. the state closest in energy. For Cr_2AlC, in-AFM2 is found +13 meV/atom higher in energy, whereas AFM$[0001]_2^X$ is found at +10 and +4 meV/atom higher energy for Cr_2GaC and Cr_2GeC, respectively. Note that the order for the three magnetic states of lowest energy of Cr_2GeC is equivalent for U_{eff} = 0 and 1. At values of U_{eff} = 2 eV, the energies of the magnetic states are well below E_0^{NM}.

Figure 1 shows the importance of including a broad range of possible spin configurations [45] when searching for the magnetic ground state. If only NM, FM and AFM$[0001]_1$ would have been accounted for, these would for U_{eff} = 0 be degenerate, and only by using the +U approach would it be possible to stabilize a state with finite local Cr moments [28, 29, 31-34, 46]. For a moderate correlation of the Cr d electrons, obtained with U_{eff} = 1 eV, in such a subset of magnetic configurations, FM would be found lowest in energy for Cr_2AC, as previously suggested in literature [28].

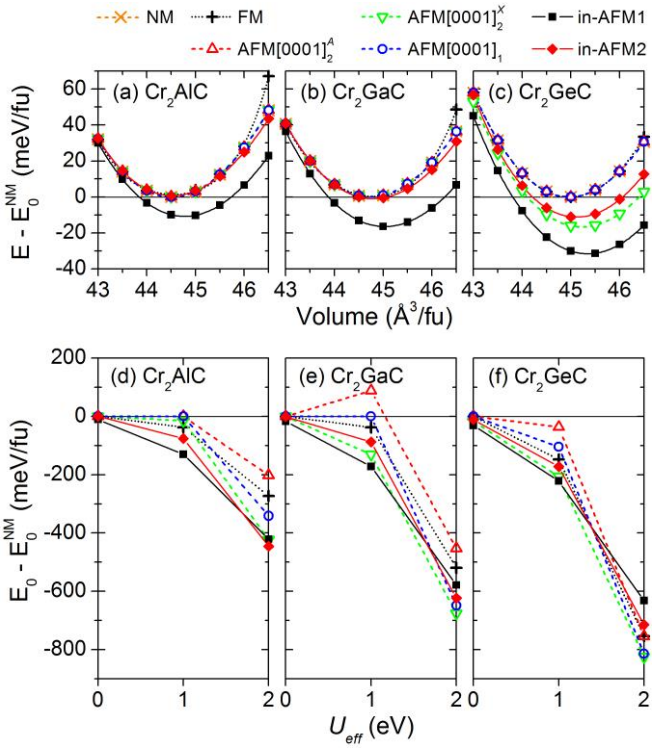

Figure 2. (Color online) (a) to (c) show total energy versus volume curves for considered magnetic states of Cr_2AlC, Cr_2GaC, and Cr_2GeC using GGA. Note that all energies are given with respect to the energy minimum of NM, E_0^{NM}. (d) to (f) show the energy difference for minimum energies E_0 of considered magnetic states relative E_0^{NM} versus U_{eff} of Cr_2AlC, Cr_2GaC, and Cr_2GeC. The considered magnetic states are NM (×), FM (+),AFM$[0001]_2^A$ (Δ), AFM$[0001]_2^X$ (▽), AFM$[0001]_1$ (○), in-AFM1 (■), and in-AFM2 (♦). The solid horizontal lines at $\Delta E = 0$ corresponds to E_0^{NM}.

Figure 3 shows the local magnetic moment per Cr atom (absolute values) versus U for considered magnetic states of Cr_2AC. In regular GGA calculations, U_{eff} = 0 eV, the local moments tend to be zero when using the 8 atoms unit cell alone (1×1×1), except for AFM$[0001]_2^X$ of Cr_2GeC. By expanding the unit cell to 2×1×1 and hence allow for in-plane AFM interactions, i.e. in-AFM1 and in-AFM2, non-zero local moments is found for all A with a magnitude from about 0.2 to 0.9 μ_B per Cr atom. For U_{eff} = 1 eV, non-zero magnetic moments is observed for all magnetic states but AFM$[0001]_1$ Cr_2AlC and Cr_2GaC. The energetically favorable magnetic configuration in-AFM1 shows an almost linear increase in moment with increasing U_{eff} for all A. This can be compared with previous theoretical studies of Cr_2AlC where NM, FM, or AFM$[0001]_1$ have been identified as low energy state [25, 28, 32]. The latter two were found only through use of the DFT+U method (U_{eff} = 1 eV) with a resulting Cr moment of 0.9 μ_B and 0.55 μ_B, respectively. Recent measurements of Cr_2AlC show a net magnetic moment of ~0.002 μ_B per Cr atom, indicating a very weak FM ordering or an

AFM state with spins slightly canted. Further studies are thus needed to reveal the magnetic structure, though the here predicted AFM ground state of these phases are within a first approximation consistent with the experiments.

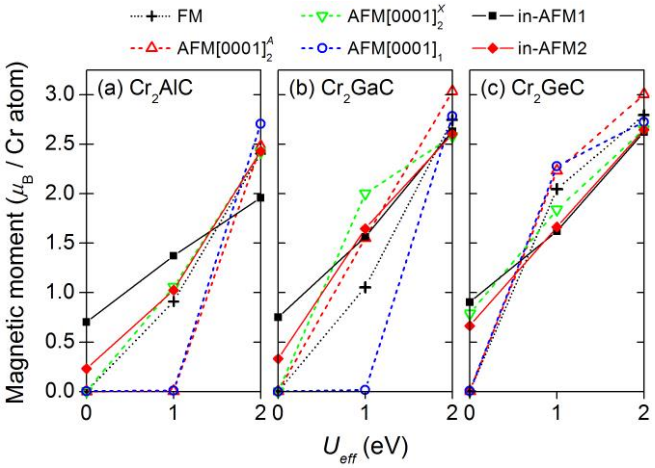

Figure. 3. (Color online) Absolute value of magnetic moment per Cr versus U_{eff} for considered magnetic states of (a) Cr_2AlC, (b) Cr_2GaC, and (c) Cr_2GeC.

The question of which approximation for electronic exchange and correlation effects that is best suited to describe a particular material is complex. In particular in a GGA+*U* framework, if the value of *U* is used as a free fitting parameter, it is important to have several different experimental observations to use as comparison. Here we use the experimentally measured *a* and *c* lattice parameters and the bulk moduli B_0 of the three different Cr_2AC (*A* = Al, Ga, Ge) MAX phases for this purpose.

The calculated lattice parameters *a* and *c* in different magnetic states and for different values of U_{eff} are given in Fig. 4. The experimental values from literature are shown as dashed horizontal lines [47-52]. For U_{eff} = 0 eV the low energy state in-AFM1 expands *a* by 0.2, 0.3, and 0.4 % and *c* by 0.2, 0.1, and 0.0 % as compared to the NM state of *A* = Al, Ga, and Ge, respectively. The calculated lattice parameters of in-AFM1 are slightly underestimating the experimental values by 0.0 to 0.3 % for *a* and by 0.6 % for *c*, with Cr_2GeC being closest. Such underestimations, although small, are not common for GGA calculations in general which instead tends to overestimate lattice parameters, in contrast to the local density approximation (LDA) which underestimates them [53, 54].

For U_{eff} = 1 eV two general observations can be made; (i) both *a* and *c* increases as compared to U_{eff} = 0 eV, and (ii) there is an increased spread of the lattice parameters since we do not any longer have degenerate states, as shown in Fig. 2. Compared to experiments, the lattice parameters of the low energy state in-AFM1 are overestimated by 0.3 to 0.7 % for *a*, and -0.1 to +0.7 % for *c*. The second

lowest energy state, in-AFM2 (A = Al), show an a identical with experiment and underestimates c by 0.4 %, For A = Ge and Ga, AFM$[0001]_2^X$, a is overestimated by +2 and +3 %, respectively. For U_{eff} = 2 eV, the calculated lattice parameters are drastically different from experimentally obtained values, e.g. about +3.5 % for AFM$[0001]_1$ Cr_2GeC. Hence, based on lattice parameters only, a reasonable value of U_{eff} for describing Cr_2AC, if necessary, should be between 0 and 1 eV.

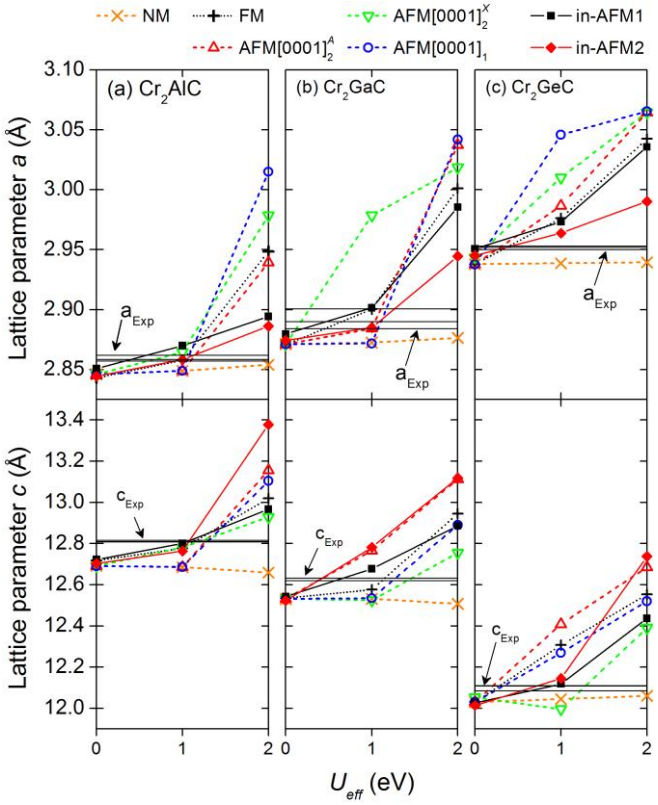

Figure 4. (Color online) Lattice parameter a (top panels) and c (bottom panels) versus U_{eff} for considered magnetic states of (a) Cr_2AlC, (b) Cr_2GaC, and (c) Cr_2GeC. Solid horizontal lines show experimental reference values for Cr_2AlC [47-49], Cr_2GaC [47, 50, 51], and Cr_2GeC [47, 49, 52].

Figure 5 shows the calculated bulk modulus B_0 versus U_{eff}. Without correlation effects, in-AFM1 were found with lowest B_0 for all A (~8 % lower than NM). Use of GGA+U results in a decrease of B_0. This decrease correlate rather well with the increased volume (a and c in Fig. 3) and resulting increase of magnetic moments in Fig. 3. The comparison of calculated B_0 with measured values is not trivial and has caused discussion in previous work for the example Cr_2AlC [28, 34, 45], Different experimental techniques give diverse results, as shown for Cr_2AlC and Cr_2GeC, where the larger values are obtained using a diamond anvil cell (DAC) [47]. For Cr_2GaC only one value was found [47]. Still, the experimental and theoretical values of B_0 for the low energy configuration in-AFM1 of Cr_2AlC and Cr_2GeC, are within 10 GPa (7%) for U_{eff} = 0 eV. For U_{eff}= 1 eV, the three magnetic configurations of lowest energy (in-AFM1, in-AFM2, AFM$[0001]_2^X$) underestimates B_0 compared to

DAC-measured values, except for in-AFM2 Cr_2AlC. In calculations using a larger value of U_{eff}, i.e. 2 eV, B_0 of in particular Cr_2GaC deviates drastically from the experimental value with an underestimation of more than 38 %. However, within this work we use a MAX phase structure with no defects or impurities, which might not reflect the experientially evaluated sample. Here performed test calculations show that *A*- and C-vacancies in Cr_2AC lower B_0 for in-AFM1 and NM, up to 5% for 12.5% vacancy concentration on the *A*- or C –site. That is, if the experimental samples would contain C- or *A*-vacancies, the discrepancies in B_0 with vacancy free GGA+*U* calculations ($U_{eff} > 1$ eV) becomes even more striking.

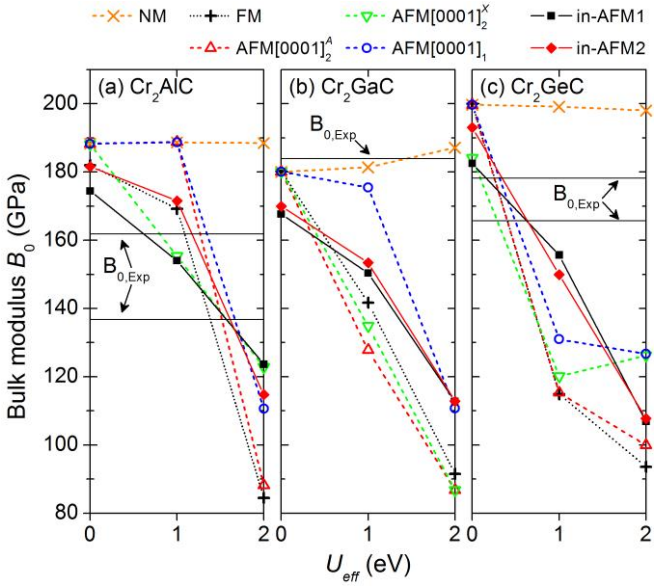

Figure 5. (Color online) Bulk modulus B_0 versus U_{eff} for considered magnetic states of (a) Cr_2AlC, (b) Cr_2GaC, and (c) Cr_2GeC. Solid horizontal lines show experimental reference values for Cr_2AlC [47, 55], Cr_2GaC [47], and Cr_2GeC [47, 52]

In Fig. 6, we present calculated density of states (DOS) for in-AFM1 Cr_2AlC using GGA+*U*, with U_{eff} = 0, 1, and 2 eV, and hybrid functionals (HSE06). For HSE06 we used the equilibrium structure of in-AFM1 Cr_2AlC obtained for U_{eff} = 1 due to calculated lattice parameters close to measured values. The peak below -10 eV corresponds to C 2*s*. Cr 3*d* – C 2*p* hybridization dominates in the range -8 to -4 eV. Above the pseudogap, i.e. the minimum in energy just above the Cr 3*d* – C 2*p* hybridization, there is Cr 3*d* – Al 2*p* hybridization. States close to the Fermi level (E_f) corresponds to non-bonding Cr 3*d* electrons. With increasing U_{eff} the localization of the Cr 3*d* electrons are gradually increased. This mainly affects Cr 3*d* states close to E_f leading to an enhanced spin polarization as seen both by the increased separation of the spin up and spin-down Cr 3*d* peaks below and above E_f and by the increased local moment of Cr. The DOS for in-AFM1 of Cr_2GaC and Cr_2GeC both show similar behavior as Cr_2AlC.

The calculated DOS and local moment obtained with HSE06 in panel (d) would here correspond to the use of $U_{eff} > 2$. Use of HSE06 on Cr_2GeC has been shown to result in Cr local moments of 3 μ_B and too large equilibrium volumes compared to experimental values (~10%) [29]. The use of hybrid functionals is known to solve issues like band gap predictions in semiconductors. However for metallic systems, such as MAX phases, its use is questionable as the exchange splitting is significantly overestimated which leads to an overestimation of the predicted magnetic moment [56].

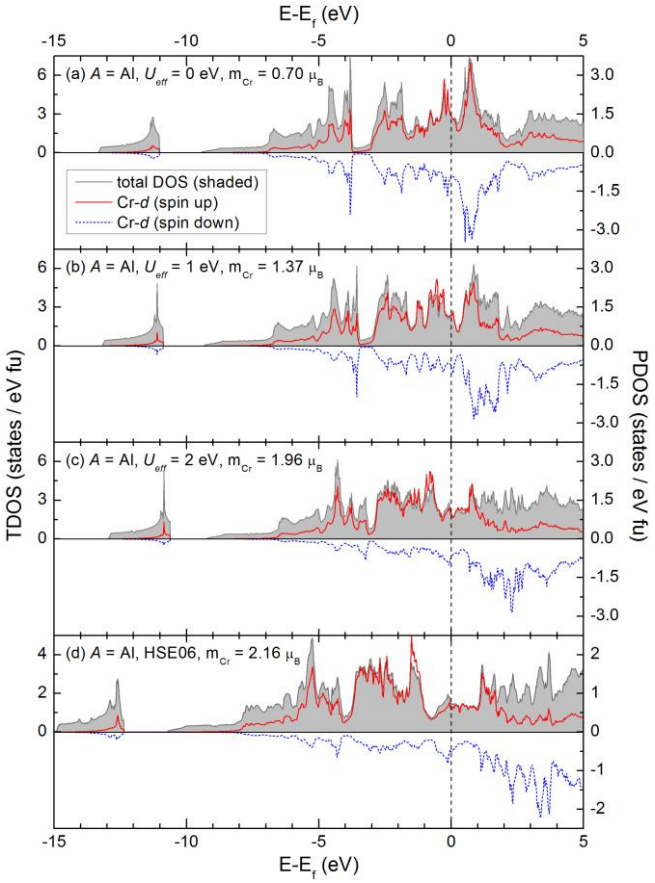

Figure 6. (Color online) Total and Cr-*d* density of states (DOS) for in-AFM1 Cr_2AlC using GGA+*U* with U_{eff}=0, 1, and 2 eV (a – c) and hybrid exchange-correlation functionals, HSE06 (d). The total DOS, partial DOS of Cr-*d* states (spin up) and Cr-*d* states (spin down) are represented by the grey shaded area, solid red line and dashed blue line, respectively. Dashed vertical line indicate the Fermi level at 0 eV.

4. Conclusions

In conclusion, we have studied the interplay of spin configuration and the approximation used for electron correlations, GGA and GGA+*U*, on the calculated lattice parameters, magnetic moments, magnetic order, bulk modulus, and electronic density of states of Cr_2AlC, Cr_2GaC, and Cr_2GeC. By considering NM, FM, and five AFM configurations, including two in-plane AFM, we show the importance of including a broad range of magnetic orders in a search for the ground state. We find

that the lowest magnetic state in all considered materials have antiparallel spins within each Cr-plane. Our calculations suggests that this class of Cr-based carbide MAX phases cannot be considered as strongly correlated systems since both GGA and GGA+*U* with $U_{eff} \leq 1$ eV gives calculated lattice parameters and bulk modulus close to experimentally reported values, if low-energy in-plane AFM magnetic states are considered. For larger values of the *U*-parameter ($U_{eff} > 1$ eV) the structural parameters deviate strongly from experimentally observed values. The lack of magnetism in theoretical investigations of Cr_2AC cannot solely be blamed on the exchange-correlation approximations, but can also be related to the magnetic orders considered. We therefore suggest that use of +*U* methods should be treated with great care until further experimental data is available to validate its significance for studies of magnetic MAX phases

Acknowledgements

The research leading to these results has received funding from the European Research Council under the European Communities Seventh Framework Programme (FP7/2007-2013)/ERC Grant agreement no. [258509]. J. R. acknowledges funding from the Swedish Research Council (VR) grant no. 642-2013-8020 and the KAW Fellowship program. B. A. is grateful for funding from the Swedish Research Council (VR) grant no. 621-2011-4417. Calculations were performed utilizing supercomputer resources supplied by the Swedish National Infrastructure for Computing (SNIC) at the HPC2N and NSC centers.

Appendix A

For completeness we also present the spin configurations used to describe FM and the five AFM configurations for M_2AX phases in table A1 and A2.

Table A1. Primitive translation vectors P_i and atomic coordinates for the 1×1×1 M_2AX unit cell used to calculate FM, AFM$[0001]_1$, AFM$[0001]_2^A$, and AFM$[0001]_2^X$ spin configurations. Spin up and spin down for individual M atoms are indicated by (+) and (–), respectively.

Type	x	y	z	Spin configuration			
				FM	AFM$[0001]_1$	AFM$[0001]_2^A$	AFM$[0001]_2^X$
P_1	$a/2$	$-a\sqrt{3}/2$	0				
P_2	$a/2$	$a\sqrt{3}/2$	0				
P_3	0	0	c				
M	$a/2$	$-a/(2\sqrt{3})$	$-zc$	+	+	+	+
M	$a/2$	$a/(2\sqrt{3})$	zc	+	–	+	–
M	$a/2$	$a/(2\sqrt{3})$	$(1/2-z)c$	+	+	–	–
M	$a/2$	$-a/(2\sqrt{3})$	$(1/2+z)c$	+	–	–	+
A	$a/2$	$-a/(2\sqrt{3})$	$c/4$				
A	$a/2$	$a/(2\sqrt{3})$	$3c/4$				
X	0	0	0				
X	0	0	$c/2$				

Table A2. Primitive translation vectors P_i and atomic coordinates for the 2×1×1 M_2AX unit cell used to calculate in-AFM1 and in-AFM2 spin configurations. Spin up and spin down for individual M atoms are indicated by (+) and (–), respectively.

Type	x	y	z	Spin configuration	
				in-AFM1	in-AFM2
P_1	a	$-a\sqrt{3}$	0		
P_2	$a/2$	$a\sqrt{3}/2$	0		
P_3	0	0	c		
M	$a/2$	$-a/(2\sqrt{3})$	$-zc$	–	+
M	a	$-2a/\sqrt{3}$	$-zc$	+	–
M	$a/2$	$a/(2\sqrt{3})$	zc	+	+
M	a	$-a/\sqrt{3}$	zc	–	–
M	$a/2$	$a/(2\sqrt{3})$	$(1/2-z)c$	+	+
M	a	$-a/\sqrt{3}$	$(1/2-z)c$	–	–
M	$a/2$	$-a/(2\sqrt{3})$	$(1/2+z)c$	–	+
M	a	$-2a/\sqrt{3}$	$(1/2+z)c$	+	–
A	$a/2$	$-a/(2\sqrt{3})$	$c/4$		
A	a	$-2a/\sqrt{3}$	$c/4$		
A	$a/2$	$a/(2\sqrt{3})$	$3c/4$		
A	a	$-a/\sqrt{3}$	$3c/4$		
X	0	0	0		
X	$a/2$	$-a/\sqrt{2}$	0		
X	0	0	$c/2$		
X	$a/2$	$-a/\sqrt{2}$	$c/2$		

[1] Wang L, Maxisch T, Ceder G 2006 *Phys Rev B* **73** 195107
[2] Hautier G, Ong SP, Jain A, Moore CJ, Ceder G 2012 *Phys Rev B* **85** 155208
[3] Aykol M, Wolverton C 2014 *Phys Rev B* **90** 115105
[4] Alling B, Marten T, Abrikosov IA 2010 *Phys Rev B* **82** 184430
[5] Botana AS, Tran F, Pardo V, Baldomir D, Blaha P 2012 *Phys Rev B* **85** 235118
[6] Alling B, Khatibi A, Simak SI, Eklund P, Hultman L 2013 *J Vac Sci Technol A* **31**
[7] Liechtenstein AI, Anisimov VI, Zaanen J 1995 *Phys Rev B* **52** R5467
[8] Dudarev SL, Botton GA, Savrasov SY, Humphreys CJ, Sutton AP 1998 *Phys Rev B* **57** 1505
[9] Petukhov AG, Mazin II, Chioncel L, Lichtenstein AI 2003 *Phys Rev B* **67** 153106
[10] Anisimov VI, Aryasetiawan F, Lichtenstein AI 1997 *J Phys Cond Matter* **9** 767
[11] Barsoum MW 2000 *Prog Solid State Chem* **28** 201
[12] Eklund P, Beckers M, Jansson U, Högberg H, Hultman L 2010 *Thin Solid Films* **518** 1851
[13] Rosen J, Dahlqvist M, Simak SI, McKenzie DR, Bilek MMM 2010 *Appl Phys Lett* **97** 073103
[14] Grünberg P, Schreiber R, Pang Y, Brodsky MB, Sowers H 1986 *Phys Rev Lett* **57** 2442
[15] Dahlqvist M, Alling B, Abrikosov IA, Rosen J 2011 *Phys Rev B* **84** 220403
[16] Ingason AS, Mockute A, Dahlqvist M, Magnus F, Olafsson S, Arnalds UB, et al. 2013 *Phys Rev Lett* **110** 195502
[17] Ingason AS, Petruhins A, Dahlqvist M, Magnus F, Mockute A, Alling B, et al. 2014 *Mater Res Lett* **2** 89
[18] Jaouen M, Chartier P, Cabioc'h T, Mauchamp V, André G, Viret M 2013 *J Am Ceram Soc* **96** 3872
[19] Lin S, Tong P, Wang BS, Huang YN, Lu WJ, Shao DF, et al. 2013 *J Appl Phys* **113** 053502
[20] Liu Z, Waki T, Tabata Y, Yuge K, Nakamura H, Watanabe I 2013 *Phys Rev B* **88** 134401
[21] Mockute A, Persson POÅ, Magnus F, Ingason AS, Olafsson S, Hultman L, et al. 2014 *Phys Status Solidi Rapid Res Lett* **8** 420
[22] Mockute A, Lu J, Moon EJ, Yan M, Anasori B, May SJ, et al. 2014 *Mater Res Lett*
[23] Tao QZ, Hu CF, Lin S, Zhang HB, Li FZ, Qu D, et al. 2014 *Mater Res Lett* **4**
[24] Jaouen M, Bugnet M, Jaouen N, Ohresser P, Mauchamp V, Cabioc'h T, et al. 2014 *J Phys Cond Matter* **26** 176002
[25] Schneider JM, Sun Z, Mertens R, Uestel F, Ahuja R 2004 *Solid State Commun* **130** 445
[26] Luo W, Ahuja R 2008 *J Phys Cond Matter* **20** 064217
[27] Zhou W, Liu LJ, Wu P 2009 *J Appl Phys* **106** 7
[28] Ramzan M, Lebègue S, Ahuja R 2011 *Phys Status Solidi Rapid Res Lett* **5** 122
[29] Ramzan M, Lebègue S, Ahuja R 2012 *Solid State Commun* **152** 1147
[30] Li C, Wang Z, Ma D, Wang C, Wang B 2013 *Intermetallics* **43** 71
[31] Li N, Dharmawardhana CC, Yao KL, Ching WY 2013 *Solid State Commun* **174** 43
[32] Li N, Mo Y, Ching W-Y 2013 *J Appl Phys* **114**
[33] Mattesini M, Magnuson M 2013 *J Phys Cond Matter* **25** 035601
[34] Du YL, Sun ZM, Hashimoto H, Barsoum MW 2011 *J Appl Phys* **109** 063707
[35] Blöchl PE 1994 *Phys Rev B* **50** 17953
[36] Kresse G, Furthmüller J 1996 *Phys Rev B* **54** 11169
[37] Kresse G, Joubert D 1999 *Phys Rev B* **59** 1758
[38] Perdew JP, Burke K, Ernzerhof M 1996 *Phys Rev Lett* **77** 3865
[39] Perdew JP, Burke K, Ernzerhof M 1997 *Phys Rev Lett* **78** 1396

[40] Anisimov VI, Zaanen J, Andersen OK 1991 *Phys Rev B* **44** 943
[41] Heyd J, Scuseria GE, Ernzerhof M 2003 *The Journal of Chemical Physics* **118** 8207
[42] Heyd J, Scuseria GE 2004 *The Journal of Chemical Physics* **121** 1187
[43] Heyd J, Scuseria GE, Ernzerhof M 2006 *The Journal of Chemical Physics* **124** 219906
[44] Monkhorst HJ, Pack JD 1976 *Phys Rev B* **13** 5188
[45] Dahlqvist M, Alling B, Rosen J 2013 *J Appl Phys* **113** 216103
[46] Sun W, Luo W, Ahuja R 2012 *J Mater Sci* **47** 7615
[47] Manoun B, Kulkarni S, Pathak N, Saxena SK, Amini S, Barsoum MW 2010 *J Alloys Compd* **505** 328
[48] Baben M, Shang L, Emmerlich J, Schneider JM 2012 *Acta Mater* **60** 4810
[49] Cabioch T, Eklund P, Mauchamp V, Jaouen M, Barsoum MW 2013 *J Eur Ceram Soc* **33** 897
[50] Etzkorn J, Ade M, Kotzott D, Kleczek M, Hillebrecht H 2009 *J Solid State Chem* **182** 995
[51] Petruhins A, Ingason AS, Dahlqvist M, Mockute A, Junaid M, Birch J, et al. 2013 *Phys Status Solidi Rapid Res Lett* **7** 971
[52] Amini S, Zhou A, Gupta S, DeVillier A, Finkel P, Barsoum MW 2008 *J Mater Res* **23** 2157
[53] Khein A, Singh DJ, Umrigar CJ 1995 *Phys Rev B* **51** 4105
[54] Lee I-H, Martin RM 1997 *Phys Rev B* **56** 7197
[55] Lofland SE, Hettinger JD, Harrell K, Finkel P, Gupta S, Barsoum MW, et al. 2004 *Appl Phys Lett* **84** 508
[56] Paier J, Marsman M, Hummer K, Kresse G, Gerber IC, Ángyán JG 2006 *The Journal of Chemical Physics* **124**